Thermal Decomposition Studies of Ammonium Heptamolybdate(6-) Tetrahydrate by Means of High-temperature Oscillating X-Ray Diffraction with a Rotating Anode Type Large Capacity Generator

Kimio Isa* and (the late) Hajime Ishimura

Department of Chemistry, Faculty of Education, Fukui University, Bunkyo 3-9-1, Fukui 910

(Received October 28, 1980)

Ammonium heptamolybdate(6−) tetrahydrate (AHM) was studied by means of high temperature oscillating X-ray diffraction with a large capacity generator of 12 kW. Experimental conditions were determined precisely. It was possible to settle the maximum value of diffracted patterns, and the inherited error was about 1.5%. Thermal decomposition of AHM was studied by means of TG-DTA, but the first decrease of TG could not be explained as a single process of decomposition. Moreover it could also not be explained by means of high-temperature oscillating X-ray diffraction with a standard generator. However, with a large capacity generator, the first decrease of TG could be explained to be a convolution of three steps of decomposition. Moreover, the second and third steps could be explained by observing the microscopic structural change. In a high-temperature oscillating XRD, (heating rate 2 °C/min), a peak temperature of 96 °C was recognized, which had not been reported before. Also from 110 °C to 226 °C, a row of the small peak has been found. Finally, the first stage of decomposition which was thought to be a single step in the experiment of TG-DTA, could be seperated into three steps. Moreover, the onset and offset temperatures of changes of characteristic diffraction intensity are determined. It was proved that high-temperature oscillating X-ray diffraction is a powerful analysing method in thermal analysis.

Thermogravimetry (TG) is defined to be a single step process as illustrated in Fig. 1.[1] We have been studying thermal decomposition of ammonium heptamolybdate-(6−) tetrahydrate ($(NH_4)_6Mo_7O_{24}\cdot 4H_2O$, AHM) in the range of room temperature to 500 °C during several years. We first measured the thermal decomposition of AHM by means of TG under an atmosphere of static air. One of the typical results is shown in Fig. 2.[2] The intermediates (a), (l), and (n) are considered to be

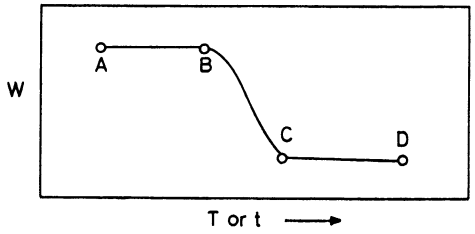

Fig. 1. TG curve of a single step process.
W, *T*, and *t* are weight change, temperature and time, respectively. AB and CD are plateaus.

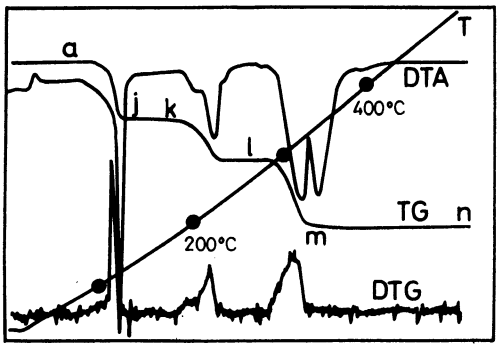

Fig. 2. One of the typical results of TG-DTG-DTA under a static air atmosphere.
Heating rate: 3 °C/min; TG full scale range: 10 mg; DTA full scale range: ±100 μV.

plateaus, but the intermediates (j), (k), and (m) are not. The steps (j) and (k) on a TG curve show gentle slopes. We must consider the gentle slopes owing either to some thermal decomposition or to an instrumental effect. From the definition of TG, the stages (j) and (k) contain multistep processes. However, this could be explained partly by DTA (differential thermal analysis). We hope to define elementary processes of this decomposition more precisely by studying the microscopic structure. The experimental methods used were mainly a simultaneous TG-DTA under various atmospheres, and a high-temperature oscillating XRD analysis (XRD: X-ray diffraction). The experimental results of the former have been already published partly.[2] The results of the latter will be discussed in this report.

The decomposition of AHM has received considerable attention as it is an isopoly anion reaction. Numerous investigators have studied thermal decompositions of AHM by means of TG, TG-DTA, powder XRD, Ω-tron mass spectrometry, and infrared absorption spectrometry, *etc.* Moreover thermal decomposition of AHM was studied by simultaneous TG-DTG-DTA-HRMS (DTG: differential thermogravimetry, HRMS: high resolution mass spectrometry) under various atmospheres (static, dry air flow, wet air flow, and (NH_3+N_2) mixture gas flow).[2,3] Recently thermal decomposition of AHM was measured by means of DSC (DSC: differential scanning calorimetry) by the authors.[4] Furthermore, by using microscopic structural analysis, we observed a phase transition occurring at 175 °C in addition to those at 110 °C, 210 °C, and 297 °C by means of high-temperature oscillating XRD with a standard X-ray generator. The conditions were: heating rate 2.5 °C/min, ranges of scanning angle, 2θ: 10.5°—13.5°, and voltage and current of the standard X-ray generator 30 kV and 30 mA, respectively. Since the intensity of the X-ray is about 800 cps and the signal-to-noise ratio at a maximum value of diffracted patterns (2θ) is about 10,

the statistical error is about 9.7%. The result of this experiment did not elucidate a gradual decrease of the TG curve. Because of a large statistical error, we could estimate neither the order of the reaction, nor the Arrhenius parameter. Then, using a rotating anode type large capacity generator thermal decomposition of AHM was measured by means of high-temperature oscillating XRD (the maximum voltage and the current are 60 kV and 200 mA, respectively). An X-ray intensity with a brilliance over 6 times as bright as a conventional hermetically-sealed X-ray tube was obtained. As the current can be varied from 10 mA to 200 mA in steps of 5 mA, the maximum peak intensity of the diffracted X-ray can be kept constant, independent of grain size, thickness of the sample, or flatness of the sample surface. In the present experiment it is possible to settle the maximum value of the diffracted pattern at 7200 cps and the inherited error is about 2%. As the maximum value of the diffracted pattern is fixed to be 7200 cps, it will be possible to determine the reaction rate of the thermal decomposition in the case of constant heating.[5]

First we considered the optimum experimental conditions of high temperature oscillating XRD. This is discussed below.

Experimental

Details of the experimental conditions are described below.

X-Ray Tube Output. Patterns of XRD are obtained by JEOL ROTEX JRX-12 using Cu $K\alpha$ radiation. Precise performances are itemized in Table 1.

Table 1. Performances of JEOL ROTEX JRX-12

X-Ray output	12 kW (Cu anode type) $\lambda_{\alpha 1}=1.54050$ Å
Maximum tube current	200 mA
Maximum tube voltage	60 kV
Focus size	0.5×10 mm^2
X-Ray tube window	10 mmϕ (Beryllium)
Tube voltage stability (input power $\pm$10% fluctuation)	0.05%
Tube current stability (input power $\pm$10% fluctuation)	0.05%
Diameter of the rotating anode type generator	100 mmϕ
Anode type species	Cu $K\alpha$

High-temperature Sample Holder. The standard sample holder of the goniometer was replaced by a high-temperature sample holder, DX-GOH-V_2(JEOL) in Fig. 3. This is made of a Pt–20%Rh alloy, and the area of the sample setting is 18×12 mm^2, the setting depth being 0.15 mm. It has a low resistance and is heated directly by a large current. Improved temperature measurements have been made using a thin thermocouple wire, Pt–Pt13%Rh, welded to the ribbon sample heater of a high temperature oscillating XRD attachement. The output signal of the thermocouple was read by a digital voltmeter (Takeda Riken Co., TR-6855) *via* a cold junction compensator. Temperature control of the hot stage is done by a controller, ULVAC-RICO PLUG-IN MODULE type THERMAL PROGRAM CONTROLLER, Model HPC-5000 Series. In Fig. 4, a 1 : 13 wounded transformer is connected between the sample holder and the controller. Intensity of diffracted X-ray signal, angle marker signals of oscillating ranges and output reading of the thermocouple are recorded by a Desk Top Recorder D-2R-1S (Ohkura Denki Co.).†

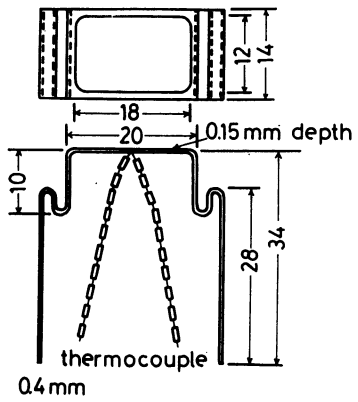

Fig. 3. A high temperature sample holder made of Pt–20%Rh alloy.

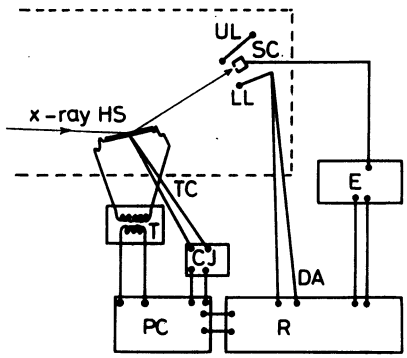

Fig. 4. An apparatus for high-temperature oscillating XRD.
HS: Hot stage; UL: upper limit switch; LL: lower limit switch; SC: scintillation counter; TC: thermocouple of Pt–Pt13%Rh; CJ: cold junction compensation; PC: thermal program controller; DA: diffraction angle; R: recorder; E: electric circuit.

Profiles of the Diffracted X-Ray Signal. Profiles of the diffracted X-ray signal are determined under the conditions described in Table 2. If more precise angular resolution that is described below is needed, the conditions shown in paren-

Table 2. Profiles of diffracted X-Ray signal

Glancing angle of X-Ray beam	4.5°
Soller slit, full opening angle	4.8°
Divergence slit	1° (1/2°)[a]
Scattering slit	1° (1/2°)[a]
Receiving slit	0.2 mm (0.05 mm)[a]
Filter species	Ni
Goniometer radius and angular accuracy	250 mm and $\pm$1/100°.

a) If more precise angular resolution of oscillating XRD is needed, the conditions shown in parentheses are used.

† In order to calibrate the linearity of the recorder, programmable DC voltage/current generator, TR-6141 (Takeda Riken K.K.), is used and its total accuracy is ± 5 μV.

theses in Table 2 are used.

Ranges of Oscillating Angles of Goniometer. The intensity of the diffracted angle, ranging between $2\theta_{low}$ and $2\theta_{high}$, is measured by high temperature oscillating XRD analysis, using limiting switches. At first usual powder XRD patterns are measured from $2\theta=5°$ to $2\theta=50°$. The angle of a maximum value of the diffracted X-ray signal is included in the range between $2\theta_{low}$ and $2\theta_{high}$. Moreover, on heating the sample in steps of 20 °C up to 500 °C, powder patterns of XRD are recorded. The angle of the highest dynamically changing value of the diffracted pattern is included in the range between $2\theta_{low}$ and $2\theta_{high}$ too. In the present case of the thermal decomposition of AHM, an angle of maximum intensity of the diffracted pattern, ($2\theta=9.7°$), is included in the range of the angle. Together with the angle of maximum intensity, more angles of strong intensity are included in the ranges of $2\theta_{low}=9.2°$ and $2\theta_{high}=13.2°$. Consequently the oscillating range of the goniometer is about 4°.

Selection of a Time Constant, τ, of the Electric Circuit. A time constant, τ, of a counting system is chosen below, *i.e.* "τ is smaller than half of the oscillation time of the slit."[6] Concerning the opening angle of the receiving slit, the goniometer scanning rate, its radius and the oscillation of the slit (described below), τ is chosen to be 0.172 s. Opening angle of the receiving slit, goniometer radius, and time width of the slit are found to be 0.0458°, 250 mm, and 0.344 s, respectively.

Conditions of the Experimental Room. In order to get rid of intensity variation due to scattering caused by the air in the path of the X-ray beam, measurements are done under the conditions of constant temperature and moisture. The present experiment is done at the constant temperature of 25 (±0.2) °C.

Heating Rate. The temperature difference, ΔT, between the temperature at an angle $2\theta_{low}$ and that at an angle $2\theta_{high}$ in the course of programmed heating, is defined by

$$\Delta T = \frac{\Delta 2\theta \cdot dT/dt}{S}, \qquad (1)$$

where S=scanning speed, dT/dt=heating or cooling rate, and $\Delta 2\theta = 2\theta_{high} - 2\theta_{low}$. In a typical experimental condition, ΔT is chosen to be 1 °C, under the conditions, $\Delta 2\theta=4°$, $dT/dt=2$ °C/min, and $S=8$ °/min.

Response of the Pen Recorder. The response of the pen recorder is 0.6 s for full scale. The half width of a peak is 5 mm and it takes 5 s to describe it. As the response time is shorter than this time, the use of this recorded for high temperature oscillating XRD is satisfactory.

Results and Discussion

Experimental Conditions. Time Constant, τ: As seen from Fig. 5 the best choice of the time constant τ is 0.1 s.

Stability of the Diffracted X-Ray Intensity: In order to examine the stability of the X-ray generator during a measurement, the intensity of the diffracted X-ray signal from the Pt-20%Rh ribbon heater versus experimental time was measured under the same conditions of the actual experiment described below, *i.e.* oscillation angle range from $2\theta_{low}=36.92°$ to $2\theta_{high}=41.17°$ and constant room temperature, during about 250 min. The peak intensity was measured versus experimental time and was averaged for during 250 min. During the first 24 min we observed a small increase of the signal of $2\theta=40.20°$ ($d=2.244$ Å), probably because the current of X-ray tube had not yet reached its stationary value. As the fluctuations of the X-ray intensity were below 1.5%, we may consider the stability of the X-ray source as fairly good.

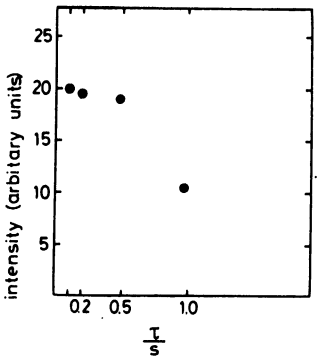

Fig. 5. Plot of intensity of XRD *versus* some time constant (τ).

High-temperature Oscillating XRD of AHM. AHM of Nakarai Co. (GR quality) was used in the form of a powder for the measurements. It was ground and sieved through standard sieves to seperate the fractions of 115—150 mesh, of 150—170 mesh and of 270—325 mesh. Moreover, for reference, a sample of Johnson-Matthey Co. of high purity (specpure chemical batch No. S84208**) was used for the measurements. In particular, in order to compare the experimental results, we mainly used samples of 150—170 mesh.

The intensity ratios of the peaks in the diffracted pattern are changed by the flatness and the thickness of the sample setting. So it is important how a sample is placed on the sample holder by a spatula, and was smoothed by a spoon. The intensity of the diffracted X-ray is about 90% of the full scale intensity (full scale is 2×10^4 cps in one case) of the recorder.

The intensity I of the characteristic X-ray is given by Eq. 2, C, A, V, and V_i are a constant, tube current, tube voltage, and exciting voltage, respectively. The intensity of the diffracted X-ray (I) of the diffraction angle, $2\theta=9.7°$ and the tube current are examined under the same experimental conditions as before. With A ranging from 10 mA to 150 mA, the relation (2) was examined experimentally. Considering I as a linear function of A : $I=aA+b$, we found by least squares method $a=0.34$ cps per Ampere and $b=1.85$ cps. Thinking b is small, it is satisfactory to use this X-ray generator for the present experiment under the conditions, mentioned above.

$$I = C \cdot A \cdot (V - V_i)^{1.5} \qquad (2)$$

In the present experiment, high temperature oscillating XRD is measured at various heating rates, 0.5, 1, 2, 3, 4, 30, and 50 °C/min, *etc.* ΔT at the various heaintg rates is presented in Table 3. For the comparison with the results of TG-DTA and DSC, the heating in the high-temperature oscillating XRD is chosen to be 2 °C/min.

A result of a high temperature oscillating XRD of

** Specification: Cu below 7 ppm, Si below 2 ppm, Ca, Fe, and Mg below 1 ppm, respectively.

Table 3. ΔT (difference of the temperature between at $2\theta_{low}$ and $2\theta_{high}$ at the various heating rates

dT/dt (heating rate) °C/min	ΔT °C	dT/dt (heating rate) °C/min	ΔT °C
0.5	0.25	4	2
1.0	0.5	30	15
2.0	1.0	50	25
3.0	1.5		

S=8°/min, $\Delta 2\theta$=4°.

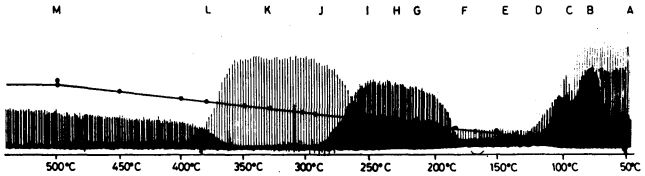

Fig. 6. One of the typical results of high-temperature oscillating XRD of AHM (115—150 mesh).
Experimental conditions: heating rate: 2 °C/min; chart spped: 5 mm/min; $2\theta_{low}$=9.37°; $2\theta_{high}$=13.43°; full scale of diffracted XRD: 1×10^4 cps; scanning speed: 8°/min; time constant: 0.1 s; divergency: 1°; receiving slit: 0.1 mm.

Table 4. Powder XRD patterns of various molybdates and molybdenum oxides in the ASTM X-Ray diffraction data files

ASTM index	Molecular formula	Crystal structure system
11-71	$(NH_4)_6Mo_7O_{24}\cdot4H_2O$	Monoclinic
18-117	$(NH_4)_4Mo_8O_{26}$	Triclinic
21-0567	MoO_3	Hexagonal
5-0508	MoO_3	Orthorhombic

AHM (150—170 mesh) at the heating rate, 2 °C/min is shown in Fig. 6. Powder XRD patterns have been collected in the ASTM X-ray diffraction data files for the compounds given in Table 4. The XRD intensities for every plane index as a function of temperature are examined precisely. In the following I_0 stand for the maximum peak intensity.

ASTM Index 11-71, $(NH_4)_6Mo_7O_{24}\cdot4H_2O$. The starting material was confirmed to be AHM by means of the standard powder XRD.

d = 9.08 Å, I/I_0 = 100, plane index (040), 2θ = 9.7°.

At about 65 °C this intensity shows a small increase and scattering becomes bigger. At about 84 °C the intensity begins to decrease drastically until about 95 °C and from that temperature it is gradually decreasing and finally at about 157 °C the peak disappears completely.

d = 7.56 Å, I/I_0 = 9, plane index (110), 2θ = 11.7°

This intensity begins to decrease from about 84 °C and disappears at about 100 °C.

d = 7.42 Å, I/I_0 = 9, plane index (110), 2θ = 11.9°

This intensity also begins to decrease from about 84 °C and disappears at about 100 °C.

d = 7.17 Å, I/I_0 = 20, plane index ($1\bar{2}1$), 2θ = 12.3°

This intensity also begins to decrease from about 77 °C and this decrease stops at about 90 °C and then it increases at about 97 °C from that temperature it begins to decrease again and at about 130 °C disappears completely.

The peak intensity of the d value, not described above, corresponding with the diffraction angle 2θ=9.7° begins to appear at about 118 °C. Moreover the peak at the diffraction angle, 2θ=13.4° begins to appear at about 110 °C and it is stable from about 124 °C to about 180 °C. From about 180 °C it begins to decrease and it disappears completely at about 226 °C.

ASTM Index 18-117, $(NH_4)_4Mo_8O_{26}$, Ammonium Octamolybdate(4−).

d = 7.21 Å, I/I_0 = 100, plane index undefined, 2θ = 12.2°.

This intensity begins to appear at about 176 °C and becomes stable at about 233 °C; it begins to decrease at about 266 °C and disappears completely at about 290 °C.

d = 9.21 Å, I/I_0 = 35, plane index undefined 2θ = 9.6°.

This intensity begins to appear at about 175 °C and becomes stable at about 200 °C. Moreover it becomes larger at about 250 °C.

ASTM Index 21-569, Hexagonal MoO_3.

d = 9.12 Å, I/I_0 = 80, plane index (100), 2θ = 9.7°.

The stable state of this peak produced from ammonium octamolybdate(4−) (AOM) is considered to be completed at about 175 °C, but at about 254 °C the peak becomes larger and becomes stable again at about 295 °C. In these temperature ranges, the intensity at the diffraction angle, 2θ=9.7°, of hexagonal MoO_3 is three times larger than that of AOM. It begins to decrease at about 355 °C and it disappears at about 405 °C.

ASTM Index 5-0508, Orthorhombic MoO_3.

d = 6.93 Å, I/I_0 = 34, plane index (020), 2θ = 12.7°.

This peak appears at about 358 °C, and becomes constant at about 426 °C. Its intensity is gradually increasing.

Meanwhile, in order to confirm an appearance temperature of maximum intensity at about 98 °C, we measured some high-temperature oscillating XRD's under the conditions described below. These conditions and the result are shown in Fig. 7.

Next, particular temperature stages of thermal decomposition are analysed by means of standard high

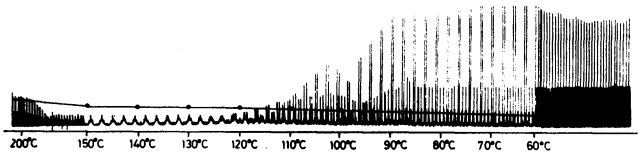

Fig. 7. One of the typical results of high-temperature oscillating XRD of AHM (115—150 mesh). Experimental conditions: heating rate: 2 °C/min; chart speed: 20 mm/min; $2\theta_{low}$=9.19°; $2\theta_{high}$=13.41°; full scale of diffracted XRD: 2×10^4 cps; scanning sped: 8°/min; time constant: 0.1 s; divergency: 1°; receiving slit: 0.1 mm.

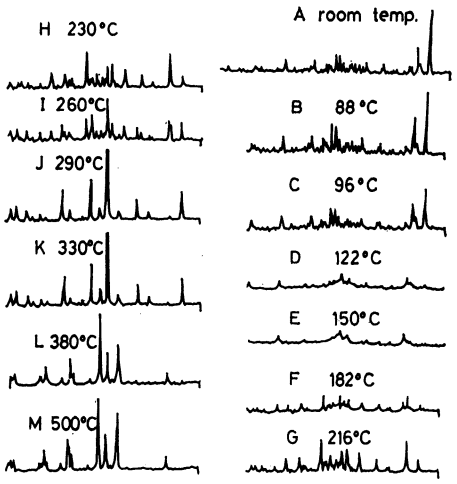

Fig. 8. The standard XRD at several temperatures.
(A) Room temperature; (B) 88 °C; (C) 96 °C; (D) 122°C; (E) 150 °C; (F) 182 °C; (G) 216 °C; (H) 230 °C; (I) 260 °C; (J) 290 °C; (K) 330 °C; (m) 380 °C; (M) 500 °C.

temperature XRD. At the desired temperature, the heating was stopped and after three minutes, the sample was cooled to room temperature, the standard powder XRD's are measured. The results are shown in Fig. 8, A)—M). The patterns of A), H), K), and M) are considered to be AHM, AOM, hexagonal MoO_3 and orthorhombic MoO_3, respectively.

Correspondence with the Results of TG-DTA and High-temperature Oscillating XRD. Thermal decomposition of AHM has been studied by E. Ma[7] and three clear steps were found to be:

$$(NH_4)_6Mo_7O_{24}\cdot 4H_2O \xrightarrow{130°C} (NH_4)_4Mo_5O_{17},$$

$$(NH_4)_4Mo_5O_{17} \xrightarrow{240°C} (NH_4)_4Mo_8O_{26},$$

$$(NH_4)_4Mo_8O_{26} \xrightarrow{360°C} MoO_3.$$

We had already studied thermal decomposition of AHM by means of TG-DTG-DTA and DSC,[2,3],†† but the upper decomposition schemes are not consistent precisely with the present experimental results. The discrepancy can be explained partly by high-temperature oscillating XRD. Before explaining the experimental results, we summarize and XRD measurement method at high temperature step by step.

I. After confirming each reaction stage by means of TG-DTA, the sample of the intermediate product is taken out from a thermobalance and measured by means of standard powder XRD.

II. At constant high temperature stage, high temperature XRD's are measured.[8] In our experiment, using a strong X-ray generator, we are enabled to take only 5 min to measure a standard XRD. It is possible to find an intermediate more easily than in case I. The reaction proceeds further, because the temperature is kept constant during 5 min, so some intermediate may happen to be missed.

III. High temperature oscillating XRD is the best analysis in order not to miss an intermediate of thermal decomposition. This method allows to find the best setting angle ranges of oscillation. Using a large capacity generator, however, the signal-to-noise ratio improve and gains better accuracy than using a standard X-ray generator. At a desired temperature during high-temperature oscillating XRD, a standard XRD is easily measured in a short time. By this improved technique, the structural changes of the precise reaction stages are observed.

Next, in comparison with a high-temperature oscillating XRD, in Fig. 2 we show a typical TG-DTG-DTA result under a static air atmosphere. The temperature of onsets and offsets of TG decrease are shown in Table 5. Also initial, final, and peak top temperatures of DTA and DSC are shown in Table 6.

Table 5. The temperatures of onsets and offsets of TG decrease

Decomposition stage	Onsets temperatures of each stage	Offsets temperatures of each stage
I	92 °C	135 °C
II	185 °C	234 °C
III	277 °C	362 °C

Table 6. The initial, peak top, and final temperatures of DTA and DSC

Decomposition stage	Initial temperature	Peak top temperature	Final temperature
I	92 °C	103 °C, 112 °C[a)]	130 °C
II	165 °C	192 °C, 217 °C[a)] (223 °C, 239 °C)[a)]	236 °C
III	256 °C	263 °C, 305 °C (329 °C)	346 °C

a) indicates the bigger peak when two peaks appear. Temperatures in the parentheses are obtained by DSC.

The results of TG showed a sharp decrease of the first stage at about 92 °C and this decrease ends at about 132°C. From this temperature TG begins to decrease gradually. At about 185 °C the second step of TG begins and at about 277 °C the third step. High-temperature oscillating XRD experiments, however, show a decrease in intensity of the (040)-plane from about 84 °C to 95 °C. This intensity finally disappears completely at about 157 °C. These two tendencies of the intensity curve (rapid and gradual) decreases of high-temperature oscillating XRD are consistent with the decreasing tendency of the first stage of TG.

Concerning the plane $(1\bar{2}1)$, two tendencies, a decreasing intensity at about 77 °C and a peak at about 97 °C, are convolved. We tried to seperate them, but did not succeed until now.

Moreover, we considered the intensity of $d=7.21$ Å of AHM, the intensity of $d=9.21$ Å of AOM and the intensity of $d=9.12$ Å of hexagonal MoO_3 from 176 °C to 258 °C. As the difference of the interplanar spacing,

†† TG-DTG-DTA was measured by means of Rigaku Co. Thermoflex, model 8002 and DSC by means of Daini Seiko Co. DSC, model SSC/560S.

d of the last two cases (*i.e.*, d=9.21 Å and d=9.12 Å) is very small, we could not seperate these two interplanar spacings. There are two possible explanations: one is a co-existance of AOM and hexagonal MoO_3, and the other one is that we simply could not seperate the peaks. In order to consider the possibility of co-existence of AOM and hexagonal MoO_3, we compare with the standard high-temperature XRD's, H) and K), at 230 °C and 310 °C, respectively in Fig. 8. Though the difference of d=9.21 Å in AOM and of d=9.12 Å in hexagonal MoO_3 is recognized slightly, we could not seperate them in a high temperature oscillating XRD. This experiment shows two stable peaks of AOM, d= 7.21 Å and 9.21 Å. At the phase transition of AOM to hexagonal MoO_3, two peaks disappear partly and a new peak, d=9.12 Å of hexagonal MoO_3 appears. In order to confirm these results, we improved the angle resolution of high-temperature oscillating XRD. Under the conditions of D=0.5°, S=0.5°, R=0.05 mm, and $d2\theta/dt$=4°/min, we could not succeed in seperating both peaks. The results also show stable temperature ranges of hexagonal MoO_3 and orthorhombic MoO_3.

The results of TG and DTA may explain the production of MoO_3 only, but whether it is hexagonal or orthorhombic MoO_3 cannot be explained by TG-DTG-DTA alone.

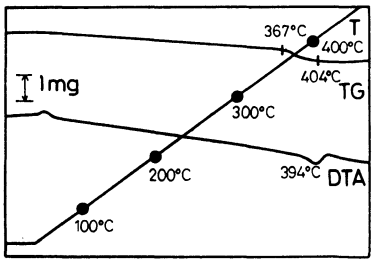

Fig. 9. Results of TG-DTA of a sample removed from the X-ray hot stage at about 330 °C, sample weight: 25.40 mg; TG full scale range: 10 mg; DTA full scale range: ±25 μV; chart speed: 20 cm/h; heating rate: 5 °C/min.

A sample of hexagonal MoO_3 was removed from the hot stage, and was analyzed by means of TG-DTA. The results are shown in Fig. 9 and two different decreasing types of TG are found. In one type the gradual weight loss of TG is about 2.4% from the room temperature to 300 °C. The other type is the rapid weight decrease of about 1.6% from 367 °C to 404 °C. Also the peak temperature of DTA is about 394 °C. The sample may not be simply MoO_3, but may be thought to be either $n\cdot(NH_4)_2O\cdot m\cdot MoO_3$ or $k\cdot H_2O\cdot MoO_3$ (n, m, k are positive integers). For the identification of this substance, a gas analysis is planned by means of simultaneous TG-MS. The weight loss of 2.4% may be due to desorption of water adsorbed by the sample after its removal from the hot stage. We conclude that the intermediate of (K) has hexagonal MoO_3 structure merely.

In X-ray spectroscopy there is always some background signal, and to decide whether or not this can be ignored is an important problem. Moreover, we must consider the accuracy of intensity measurements in high-temperature oscillating XRD. The statistical error depends on the peak intensity. If we define the number of signal intensity and of back ground as N_p and Nb, respectively, the statistical error $\sigma(\%)$ is given by the equation,[9]

$$\sigma(\%) = \frac{1}{\sqrt{Np}} \cdot \frac{\sqrt{1+Nb/Np}}{(1-Nb/Np)} \cdot 100. \qquad (3)$$

In the present experiment, Np and Nb are found to be 7040 cps and 440 cps, respectively, with σ=1.35%. For a standard X-ray tube (30 kV and 30 mA), Np and Nb were 650 cps and 70 cps, respectively, with now σ= 4.62%. Obviously the present experiment has a better accuracy, which enables to analyze a reaction rate and to determine Arrhenius parameters.

Table 7. The results of oscillating high temperature XRD

Decomposition stage	Temperature range of intensity plateaus	Cross point temperature
5 mm/min chart speed		
I_1	room temp—84 °C	89 °C
I_2	96 —100 °C	126 °C
I_3	128 —177 °C	183 °C, 187 °C
II	232 —251 °C	265 °C
III	295 —345 °C	384 °C
20 mm/min chart speed		
I_1	room temp—77 °C	99 °C
I_2	102 —104 °C	126 °C
I_3	129 —174 °C	183 °C, 187 °C

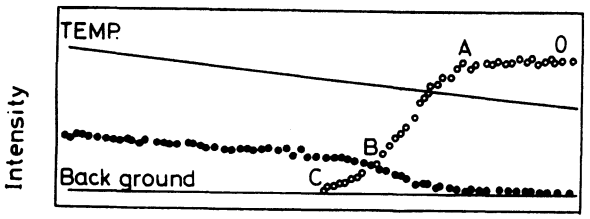

Fig. 10. Model of the result of high-temperature oscillating XRD. In the range OA one structural substance is present. In the range AC a mixture of more structural substances is present.

An appearance, disappearance, and cross point temperatures of the intensity of the diffraction patterns, are shown in Fig. 10. Moreover OA in Fig. 10 is considered to be a range of spacing versus sample temperature under programmed heating. From these measurements we may conclude that in the temperature range OA in Fig. 10, there is only one structural substance, but in the range AC, there is a mixture of structural substances. Finally we could measure points A and C more sharply by this experimental method. Consequently high-temperature oscillating XRD will become one of the most important methods of thermal analysis.

Some other inorganic salts (salts of isopoly acid) will be analyzed by high-temperature oscillation XRD method in future.

Summary

Thermal decomposition of AHM was measures by means of high-temperature oscillating XRD with a rotating anode type large capacity generator. This method enables us to measure microscopical structural changes in the field of thermal analysis. Especially, with improved S/N ratio, it is easy to determine the temperature of a phase transition and a reaction rate constant.

In a high-temperature oscillating XRD of AHM with the heating rate 2 °C/min, a peak temperature of 96 °C was found, which has not been reported before. Also from 110 °C to 226 °C, a series of small peaks was found. Finally, one stage of decomposition which was obtained in TG-DTA experiments, was seperated into three steps. The stability ranges of AOM, hexagonal MoO_3, and orthorhombic MoO_3 were clarified.

The X-ray generator is situated in the Research Institute for Material Science and Engineering, Fukui University. The author wishes to thank Professor Tohgoro Matsuo and Mr. Shigeru Hashiya for convenience of using their X-ray generator. The assistance of Miss Masayo Yoshimen during the early experiments is also acknowledged. The author would like to thank Dr. A. J. H. Boerboom and Dr. G. Harkvoort for critical reading of the manuscript. This work was partly supported by the Grant-in-Aid for Scientific Research from the Ministry of Education, Science and Culture.

References

1) G. Lombardi, "For Better Thermal Analysis," International Confederation for Thermal Analysis (1977).
2) K. Isa, Y. Hirai, and H. Ishimura, *Proc. of the 5th Int. Conf. on Thermal Analysis* (*Kyoto*), 348 (1977).
3) H. Ishimura and K. Isa, *Proc. of the 5th Int. Conf. on Thermal Analysis* (*Kyoto*), 488 (1977).
4) Unpublished.
5) Unpublished.
6) H. P. Klug and L. E. Alexander, "X-Ray Diffraction Procedures," John Wiley and Sons (1954).
7) E. Ma, *Bull. Chem. Soc. Jpn.*, **37**, 649 (1964).
8) P. F. Konovalov, A. I. Efremov, and B. V. Volkonskii, "Ionization X-Ray Equipment for Research on Crystalline Materials at Various Temperatures," (1958).
9) "Practical X-Ray Spectroscopy," ed by R. Jenkins and J. L. de Vries, Philips Technical Library, Macmillan (1972), Chap. 5, p. 90,